



### Research Article

## A PRECISE FAULT LOCATION SCHEME FOR LOW-VOLTAGE DC MICROGRIDS SYSTEMS USING MULTI-LAYER PERCEPTRON NEURAL NETWORK

Ali ABDALI\*<sup>1</sup>, Kazem MAZLUMI<sup>2</sup>, Reza NOROOZIAN<sup>3</sup>

<sup>1</sup>University of Zanjan, Department of Electrical Engineering, Zanjan-IRAN; ORCID:0000-0002-8735-6207

<sup>2</sup>University of Zanjan, Department of Electrical Engineering, Zanjan-IRAN; ORCID:0000-0002-6938-2022

<sup>3</sup>University of Zanjan, Department of Electrical Engineering, Zanjan-IRAN; ORCID:0000-0001-8085-3860

Received: 16.04.2018 Revised: 27.08.2018 Accepted: 06.09.2018

### ABSTRACT

Nowadays, microgrids have attracted much attention in developed countries. The protection of DC systems, unlike conventional AC systems, is a highly challenging task. The acquaintance on fault location in distribution network causes for quick restoration, maintenance and decrease unnecessary power outage period. Neural Networks (NNs) are among the powerful, reliable approaches and are used in many different engineering applications. Also, Multi-Layer Perceptron (MLP) NNs are used for different estimating problems. This paper presents an accurate protection method for Low-Voltage DC (LVDC) ring-bus microgrid systems based on MLP NN. The aim of the proposed method is precise fault location estimation in microgrids, irrespective of the type and magnitude of fault, current, and the power supply quantity, by instantaneous current monitoring of each segment of the microgrid. Simulation results demonstrate the NN fault location estimation in percent of line length are in a suitable range. The results show that the estimation error is small and is within the permissible range. According to the results, efficiency and accuracy of MLP NN are confirmed. To do so, an LVDC ring-bus microgrid is used that utilizes solid-state bidirectional switches along with master and slave controllers

**Keywords:** Fault location, neural network (NN), multi-layer perceptron (MLP), low voltage DC (LVDC) microgrids, solid-state circuit breaker.

### 1. INTRODUCTION

A great number of studies have recently been conducted to develop and arrive at favorable conditions of utilizing renewable energy resources for instance wind and solar energy in the electrical energy distribution networks. Additionally, distributed generation systems have advantages over traditional power generation procedures at centralized power plants due to their higher reliability and performance, environmental compatibility and easier controllability [1], [2]. Microgrid systems are small-scale power grids that consist of renewable energy resources and loads [3]– [5].

Microgrids can be utilized in two modes, islanded and grid-connected modes. Microgrids may generally be categorized into DC and AC systems. The advantage of AC microgrids is the

\* Corresponding Author: e-mail: ali\_abdali@znu.ac.ir, tel: +989102030445

possibility of using distributed generation sources directly which are based on AC voltages; however, synchronization, reactive power control, and voltage stability are among their disadvantages. Nevertheless, DC microgrids are considered to be a feasible solution, since they are small grids with less transmission losses. Moreover, they lack the defects of AC systems, and the size of AC-DC-AC converters used may be significantly reduced.

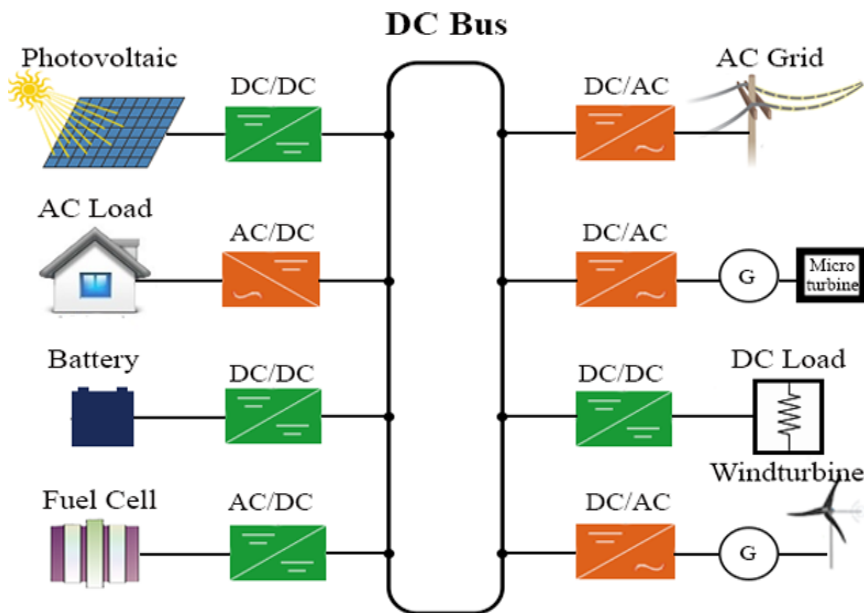


**Figure 1.** Conceptual scheme of an LVDC ring bus microgrid.

Fig. 1 shows a conceptual scheme of an LVDC ring-bus microgrid. LVDC systems, contrary to HVDC ones, are the more recent concept in power distribution networks. For small-scale systems, LVDC microgrids offer plenty privileges over AC classical networks. AC and DC microgrids need power electronic converters and are used to link loads and resources to a common bus. Therefore, the use of DC microgrids requires less converters [6] - [8]. In addition, cables utilized in power systems are chosen depend on the peak voltage of the system. The maximum transferred power in AC systems depends on the rms value, whilst in DC systems it is based on maximum voltages. Therefore, the DC system can transfer  $\sqrt{2}$  times more than one AC system with the same cable. The DC system is not affected by the phenomenon of skin effect and can use the entire cable, which decreases transmission power losses [8], [9].

Despite their significant advantages, the protection of DC microgrids poses many challenges and, as well as, no written standards, solutions, or experience exist in regard to this topic [7]. In the distribution system, the capability of precise fault location provides advantages such as quick repair, maintenance, and restoration, leading to reduced duration of power interruptions [6], [10]. The DC systems boost power flow, power quality and equipment size and weight using power electronic converters. Attendance of power electronic equipment controls current to a certain extent during fault conditions, which intern make fault location difficult [11].

It is not common to set up protection devices at the DC section of microgrids and, circuit breakers (CBs) in the AC system are activated in the fault condition. Accordingly, a procedure has been suggested in [12] to separate the faulted section. Notwithstanding, this scheme entirely de-energizes the DC section. This method is suitable for HVDC and MVDC systems that work as

link interconnecting two AC systems. This method causes an unnecessary outage of sources and loads in DC microgrids. Various fault protection solutions have been proposed for LVDC distributed systems including overcurrent protection [7]– [9], derivatives of current [7], under-voltage and directional protection [8]. Nevertheless, the dynamics of voltage and current in the faulted segment were not considered. A fault detection method based on traveling waves was proposed in [13] for multi-terminal DC (MT-DC) systems.

A differential method of fault detection and isolation in LVDC bus microgrids was proposed in [14]. The disadvantage with this method is the use of a specific threshold for fault detection, meaning that the fault occurs when line current exceeds the threshold. Obviously, fault detection speed depends on this threshold value, which is a defect.

The present research aims at correcting the aforementioned defect of the [14], so that human actions and considerations would not affect fault detection. The advantage of the present paper is that the protective algorithm does not depend on human actions and consideration and is fully intelligent. In this paper firstly, multilayer perceptron (MLP) neural network (NN) is employed to estimate the fault location distance.

## 2. LV DC MICROGRID

LVDC networks, contrary to HVDC ones, are the more recent approach in distribution networks. Stable, versatile protection is the current challenge of DC systems. Compared to AC systems, more experience and various standards are available concerning the protection of AC systems. Fuse and CBs are the available protection equipment for DC systems [8]. CB mechanisms used in AC systems operate when fault current crosses zero. However, this mechanism is not applicable to DC systems. More importantly, the circuit breaker is activated after a longer period of time, causing a fault to exist for a longer duration, that this is highly catastrophic for DC systems.

### 2.1. Faults in DC Microgrids

Two types of faults may occur in DC microgrids as demonstrated in Fig. 2:

- 1) Line to line fault
- 2) Line to ground fault.

A line to line (or pole to pole) fault is one where short-circuit occurs between positive and negative lines in a system, while a line (or pole) to ground fault is one where a short circuit occurs between one line (or pole) of the system, positive or negative, and the ground. This is the most usual kind of faults in distribution systems [15].

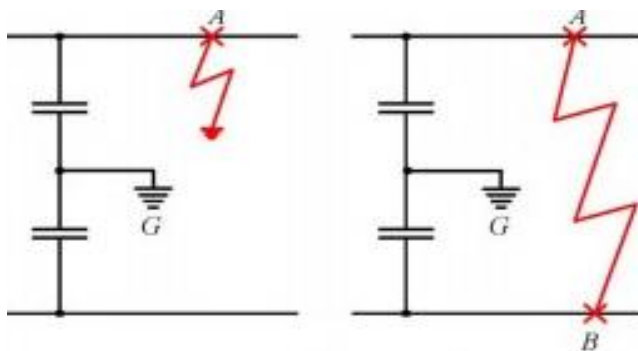


Figure 2. Two feasible faults in DC microgrids.

## **2.2. Available protection equipment for DC systems**

In this section, available protection equipment for DC systems is mentioned. Because of the restrictions of fuses and AC Circuit Breakers (CBs) in DC systems, a solid-state CB is considered as an appropriate choice for DC system protection. There exist different options including GTO, IGBT, and IGCT, among which IGCTs offer effective and better performance [16]- [19].

In DC microgrid bus, due to that let power flow in bi-side, the aforementioned CBs must be bidirectional. Another equipment to protect the network from extra fault currents is taking advantage of fault current limiters (FCLs) in fault condition. Advantages of FCLs include the higher capability to ride-through for temporary faults, reduction of short circuit level of CBs, network losses and costs. Various limiters have been proposed so far including superconductors [20], saturated inductors [21] and power electronic equipment [22].

## **3. THE PROPOSED FAULT LOCATION SCHEMES USING MLP NN**

In this section, the proposed controller and fault location based on MLP NN are presented.

### **3.1. The proposed controller**

In this paper instead of a complete system shutdown or DC-bus current limiting, the fault is first detected and then isolated from the system and to allow the rest of the system to keep operating. To this end, a loop-type common DC bus is employed to make the microgrid robust in faulted condition (Fig. 1 and Fig. 6). It was also shown that loop-type systems were more efficient, particularly when transmission lines were not very long [14]. The total loop type bus is segregated into a series of sections. Every segment includes a section of the bus and a segment controller. A schematic of the protection method is depicted in Fig. 3. The suggested protection scheme contains one master controller, two slave controllers and freewheeling branches between all pole and the ground. Slave controllers measure current values at the two ends of the bus section and transmit them to the master controller. The slave controllers were also responsible for the execution of control commands sent from the master controller for the switching of freewheeling branches. In regular circumstances, measurements at each end of bus section must be identical, and the master controller sets the pole CBs in close mode.

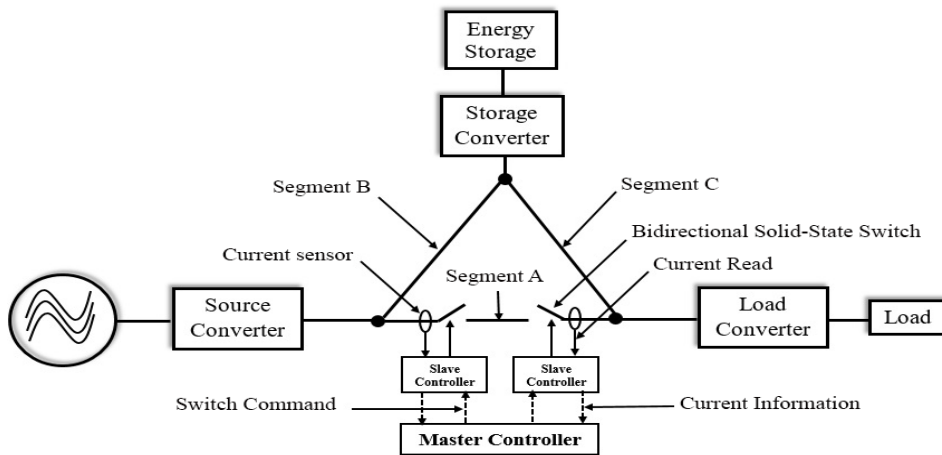


**Figure 3.** Schematic of the suggested protection structure (similar controllers also exist in segments B and C).

### 3.2. Implementation of MLP NN

In this section, the objective is fault location of the respective zone after fault detection. NNs are among the powerful and reliable approaches and are also used in many different engineering applications and problems to estimate promising results [23]. Since fault location is an estimated problem, the estimating tools were used to estimate the fault location. Neural networks with their high ability to deduce results from complex data can be used to extract patterns. There are different neural networks such as RBF, RNN, MLP, DNN, etc. For which the structural differences between the neural networks, and both the nature and structure of the problem should be taken into account. Multilayer perceptron (MLP) neural networks are able to make a nonlinear mapping with an excellent accuracy by choosing the appropriate number of layers and neural neurons, which is what we are seeking for.

As stated, the amplitude of the fault current is inversely correlated with the impedance of the fault current path, i.e. if the impedance increases, the fault current decreases and vice versa. Therefore, the relationship between the fault location and the fault impedance path can be expressed by a nonlinear mapping. Because the MLP neural network performs nonlinear mappings with lower computational bulk and complexity as well as with sufficient accuracy, the MLP neural network is used to estimate fault location.

What is an ANN? ANN is a data progressing system inspired by biological neural systems, e.g. human brain, to analyze information. The system is comprised of fully integrated processing elements known as neurons that cooperate in parallel to solve a problem. In other words, ANNs are novel computational systems used in machine learning applications to find a way to represent and eventually implement knowledge in order to predict output responses of complicated systems. ANNs, along with programming knowledge, are used to design a data structure simulating nerve cells in the brain.

Why do we use ANNs? Relying on their outstanding capabilities in inferring results from complicated data, ANNs can be used to extract and identify patterns that humans and computers find difficult to identify.

### 3.2.1. Properties of NNs

Properties of NNs include adaptive training, self-organizing, real-time operators, fault tolerance, and, generalization [23].

- *Transfer (stimulus) functions*

The transfer function  $f()$  is determined based on the specific requirements of a problem. The transfer function may either be linear or nonlinear. Some important instances of transfer functions are pointed out as follows:

a) Linear transfer function: As demonstrated in Fig. 4(a), the function output is equal to its input.

b) Sigmoid transfer function: The sigmoid function is generally represented by the following equation [20]:

$$F(x) = \frac{1}{1 + e^{-cx}} \quad . c > 0 \tag{1}$$

For  $c=1$ , the figure of the function is demonstrated in Fig. 4(b). The value  $c$  determines the extent of the linear region.

c) Hyperbolic tangent transfer function: It is an odd and asymmetric function. Experience has shown fast training of NNs with this function. The function equation is as follows:

$$F(x) = a_0 \tan b_x \tag{2}$$

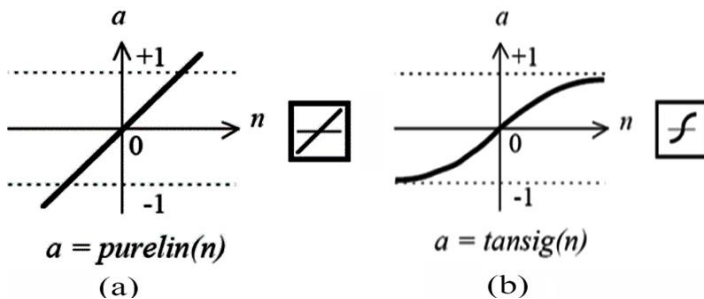


**Figure 4.** Linear transfer function(a), Sigmoid transfer function(b).

MLP NNs are often formed by a number of single layers cascaded together, where the output of each layer is fed into the next. Every layer contains a specific weight matrix 'w', a bias vector 'b', a net input vector 'n', and an output vector 'a'. A 3-layer feedforward MLP NN is demonstrated in Fig. 5. As can be seen, the number of inputs and neurons in the first layer of the 3-layer MLP feedforward NN are 'R' and 'S', respectively.

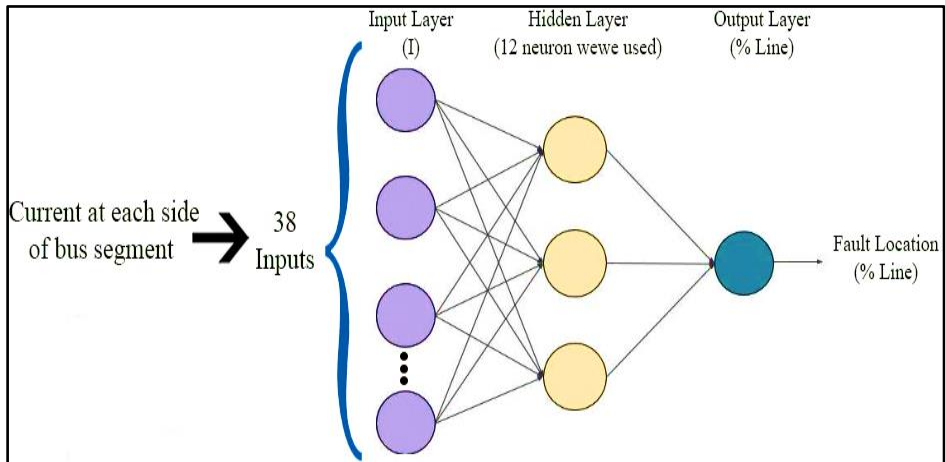


Figure 5. 3-layer MLP feedforward NN.

### 3.2.2. The selected structure based on NN

The selected structure of MLP is a 3-layer network, which has a lower computational bulk and complexity as well as sufficient accuracy in fault location estimation:

a) Input layer: This layer is responsible for processing input signals to the NN and uses interlayer coefficients to send output signals to the next layer. The number of neurons in this layer is equal to the number of input variables ( $I_{in}$  and  $I_{out}$ ).

b) Hidden layer: In this paper, to cover all possible states, the hyperbolic tangent transfer function is used in analyzing system conditions and making appropriate decisions accordingly. The number of neurons in this layer may change, and the larger the number of neurons the more the processing power of the NN. There is always a trade-off between duration and computational costs, as well as the required accuracy. In this study, 12 neurons are considered for the hidden layer.

c) Output layer: The processed data in the hidden layer is sent to the output layer after it is transformed into the appropriate commands and signals. In this paper, the output of the hidden layer is the length percentage of the transmission line, where a fault has occurred. A linear transfer function is employed in this layer.

### 3.2.3. Training MLP NN

In order to train the NN for achieving the suitable estimation accuracy, a database is first prepared. To this end, the microgrid in the previous section is simulated with different faults at different locations. Short circuit fault is applied to different line segments, from  $d=5\%$  to  $d=95\%$  (in steps of 5%) of the line length, and the corresponding fault currents are measured to be stored in a database matrix. Then the prepared database is used to train the NN. For the fault location using MLP NN,  $I_{in}$  and  $I_{out}$  currents are selected from each segment as a database. Then, it was used for offline training. The offline training of the MLP is carried out with the Error Back Propagation (EBP) method by the Levenberg-Marquardt (LM) algorithm. As well as, in the training epoch the number of iteration is considered 1000.

Many efforts have been made to speed up EBP algorithm. All of these methods lead to little acceptable results. The Levenberg-Marquardt (LM) algorithm [24], [25] ensued from development of EBP algorithm dependent methods. It gives a good exchange between the speed

of the Newton algorithm and the stability of the steepest descent method [26], that those are two basic theorems of LM algorithm.

In the EBP algorithm, the performance index  $F(w)$  to be minimized is defined as the sum of squared errors between the target outputs and the network's simulated outputs, namely:

$$F(w) = e^T e \tag{3}$$

Where  $w = [w_1, w_2, \dots, w_N]$  consists of all weights of the network,  $e$  is the error vector comprising the error for all the training examples. When training with the LM method, the increment of weights  $\Delta w$  can be obtained as follows:

$$\Delta w = [J^T J + \mu I]^{-1} J^T e \tag{4}$$

Where  $J$  is the Jacobian matrix,  $\mu$  is the learning rate which is to be updated using the  $\beta$  depending on the outcome. In particular,  $\mu$  is multiplied by decay rate  $\beta$  ( $0 < \beta < 1$ ) whenever  $F(w)$  decreases, whereas  $\mu$  is divided by  $\beta$  whenever  $F(w)$  increases in a new step. The standard LM training process can be illustrated in the following pseudo-codes,

1. Initialize the weights and parameter  $\mu$  ( $\mu = .01$  is appropriate).
2. Compute the sum of the squared errors over all inputs  $F(w)$ .
3. Solve (2) to obtain the increment of weights  $\Delta w$
4. Recomputed the sum of squared errors  $F(w)$

Using  $w + \Delta w$  as the trial  $w$ , and judge

IF trial  $F(w) < F(w)$  in step 2 THEN

$$w = w + \Delta w$$

$$\mu = \mu \cdot \beta \quad (\beta = .1)$$

Go back to step 2

ELSE

$$\mu = \mu / \beta$$

go back to step 4

END IF

#### 4. SIMULATION RESULTS

A case study microgrid is depicted in Fig. 6. The simulation circuit includes the exact model of wind turbine, exact model of photovoltaic cell, short line model with dispersed capacitors, freewheeling branches for fault current damping, bi-directional IGBT switches, antiparallel diodes of the IGBT switches, RCD snubber circuit to suppress voltages overshoot due to the line inductance effect, model of DC and AC loads, energy storage model, two-level VSC and DC/DC converters, the power electronics converters' DC link capacitors, VSC-based DC/AC converter, etc. Different segments are named as segA, segB, and segC. The voltages of DC supply sources in all segments are assumed to be 240V, and the simulated network is TN grounded. Each segment of the DC bus is a 0.2km cable and specification of the simulated sample are exploited from [14], [27]. The snubbers employed are of RCD type [28]. In the simulations, the delays of switching and communication were neglected but the effect of these delays has been considered in the practical implementation section.



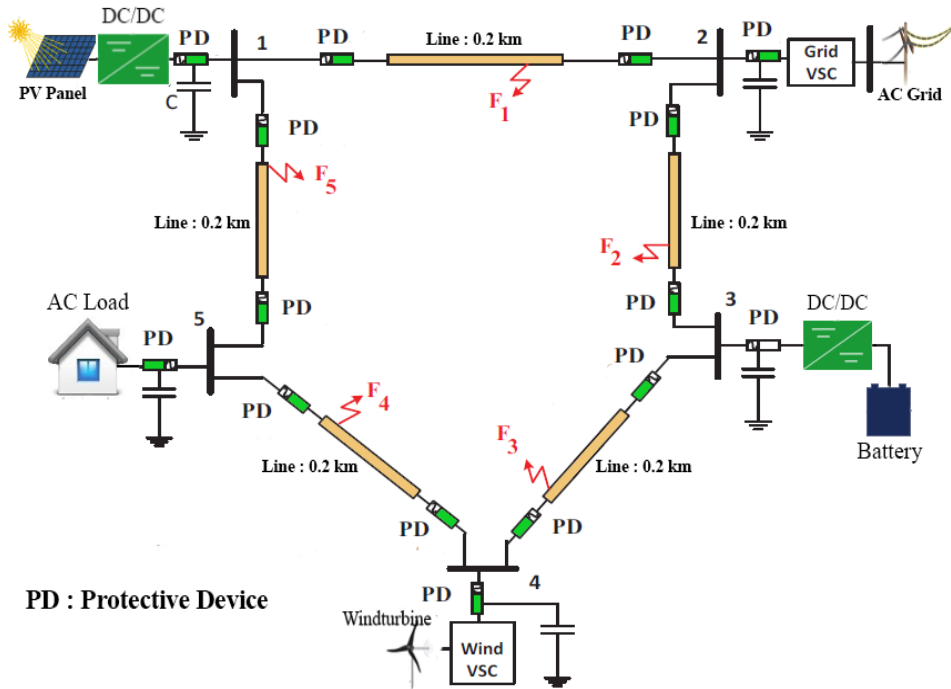


Figure 6. LVDC ring-bus microgrid architecture considered in this study.

#### 4.1. Fault location estimation using MLP NN

In this section, an MLP NN model is added to the microgrid simulation. The model uses normal distribution function to normalize the input data. The normal distribution function is defined according to the mean value and variance of data as follows:

$$f(x, \mu, \sigma^2) = \frac{1}{\sigma\sqrt{2\pi}} \exp\left(-\frac{(x-\mu)^2}{2\sigma^2}\right) \quad (5)$$

After simulating the MLP NN, it is trained with the prepared database of different microgrid faults. Root Mean Square Error (RMSE) criterion is used to assess the training efficiency of the NN. The RMSE represents the error between real values from the database and the estimated values in each training epoch. In other words, the estimation error of all the data is equal to RMSE percentage:

$$RMSE\% = 100 \times \sqrt{\frac{1}{N} \sum_{i=1}^N (y_i^{estimated} - y_i^{real})^2} \quad (6)$$

Where N is the whole number of training data. Smaller RMSE values mean higher accuracy of the NN in estimating objective function and the appropriate efficiency of the training process. Fig. 7 shows the convergence graph of the NN training.

As can be seen in Table 1, in the training epoch the correlation between the estimated values and real value is 97.5%, and the maximum error between them is 5%. Following the training epoch, no real values are provided to the NN, and outputs are estimated based on the input values. The test algorithm then updates NN weights according to the estimation error. In the next epoch, the NN is only assessed by receiving inputs that are not previously provided to the NN. Then, the estimated outputs are assessed based on the corresponding inputs, but no weights are updated in

this epoch. If the NN performance is not approved, training should be performed again from the beginning. The performance of NN in the assessment epoch is very promising. The MLP NN estimates fault location with a maximum error of 1.6%. Fig. 8 demonstrates the correlation graph between the real values and the estimated results. As can be observed, the maximum estimation error of 1.6% may only happen if the fault occurs in the first and last 20% of the transmission line length; whereas in other regions of the line, fault location is estimated almost accurately.

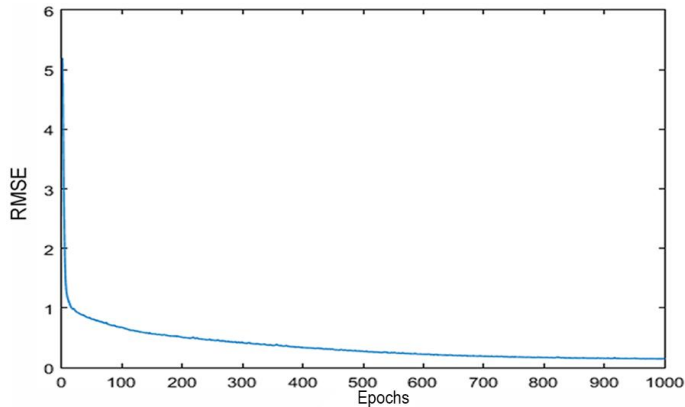


**Figure 7.** Convergence graph of the training algorithm.

**Table 1.** Accuracy and Validation Results of Assessing the MLP NN

Epoch	Correlation coefficient	Maximum calculation error
Training	97.5%	5%
Test	98.3%	3.8%
Assessment	98.9%	1.6%

Simulated model of MLP neural network in “MATLAB/Simulink” software is demonstrated in Fig. 9. The detailed description of the neural network is as follows.

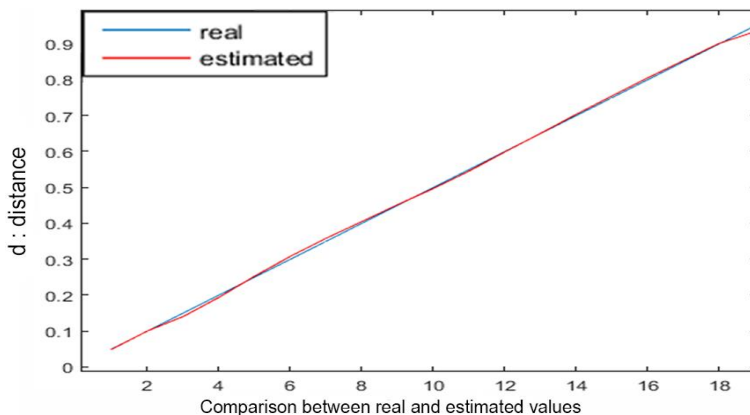


**Figure 8.** Correlation between real and estimated results.

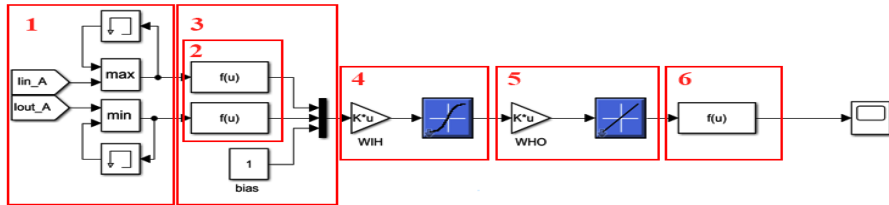


**Figure 9.** Simulated model of MLP neural network in “MATLAB/Simulink” software.

- Section 1: In this section, the input and output current are measured at each instant and the maximum value is extracted by comparison with the pre-current size.
- Section 2: After extraction of the maximum error of current in the two sides of the line, data is normalized with the help of "mux" and "sigmax" values. This function is written as a function in blocks  $f(u)$ .
- Section 3: After the current values normalizing, along with the Bias, a network input vector is formed, using the "mux" the three values in a vector as output is considered.
- Section 4: By using the matrix multiplication in the Gain block, the coefficient weight matrix between the input and the hidden layer is multiplied by the input vector and the sigmoid tangent transfer function is applied to it.
- Section 5: The output of the hidden layer is multiplied by the weight matrix between the hidden layer and the output layer and passes through the linear transfer function. The output of this section is estimated value of the neural network.
- Section 6: The estimated value of the hidden layer is removed from the normal distribution space by the "muy" and "sigmay" vectors and converted to the amplitude of the power system.

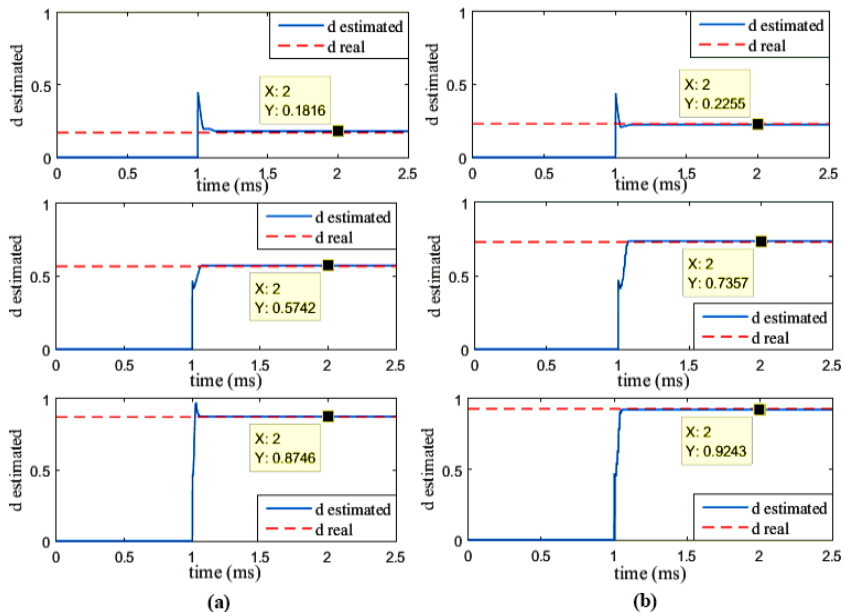


**Figure 10.** Estimation of LL short circuit fault location in 17%, 57% and 87% of the line length (a) and estimation of LG short circuit fault location in 23%, 73% and 93% of the line length (b).

For a better representation of NN capabilities, 6 different simulation conclusions are demonstrated in Fig. 10. Fig. 10(a) depicts calculations of the fault location estimation for an LL fault occurring at 17%, 57% and 87% of the line length measured from the source side, respectively using the MLP NN. As can be seen from the Fig. 10(a), the designed NN estimated the fault at 18.16%, 57.42% and 87.46% of the line length, respectively. The estimation errors for both states are calculated as 1.16%, 0.42%, and 0.46 %.

Fig. 10(b) shows the estimation of the NN for an LG short circuit when the assumed fault is applied to a 46m, 146m and 186m distance from the source side in segA, respectively. The designed NN estimated the fault at 22.55%, 73.57% and 92.43% of the line length, respectively. In other words, the MLP estimation was 45.1m, 147.14m and 184.86m distance from the source side, respectively. The estimation error was calculated as 0.45%, 0.57% and 0.57% or 0.9m, 1.14m and 1.14m, respectively.

For further assessment of proposed MLP NN, Table 2 is provided. Table 2 is the result of fault location estimation using MLP NN for LG and LL short circuit. The results show that the estimation error is small and is within the permissible range. According to the results, efficiency and accuracy of MLP NN are confirmed.

**Table 2.** Fault location Estimation

Fault distance in % of line length from the source (Fault type)	Fault distance from the source(m)	Distance estimation in % of line length	Distance estimation(m)	Estimation error
0.02 (LL)	4	0.0151	3.02	0.0049
0.08 (LG)	16	0.07912	15.824	0.00088
0.1 (LG)	20	0.09296	18.696	0.00702
0.19 (LL)	38	0.1989	39.78	0.0089
0.21 (LG)	42	0.2069	41.38	0.0031
0.26 (LL)	52	0.2599	51.98	0.0001
0.32 (LL)	64	0.313	62.6	0.007
0.38 (LG)	76	0.3843	76.86	0.0043
0.43 (LL)	86	0.4277	85.54	0.0023
0.49 (LG)	98	0.4871	97.42	0.0029
0.51 (LG)	102	0.5085	101.7	0.0015
0.56 (LL)	112	0.563	112.6	0.003
0.63 (LL)	126	0.6325	126.5	0.0025
0.66 (LG)	132	0.6615	132.3	0.0015
0.72 (LG)	144	0.7217	144.34	0.0017
0.79 (LL)	158	0.7926	158.52	0.0026
0.84 (LG)	168	0.8409	168.18	0.0009
0.88 (LL)	176	0.8863	177.26	0.0063
0.98 (LL)	196	0.9813	196.26	0.0013

## 5. CONCLUSION

This research proposed a novel fault location scheme for LVDC ring-bus microgrids. The proposed protection method is based on NN which are able to estimate fault locations more quickly as soon as possible. According to the results, the accuracy and efficiency of fault location method based on MLP NN are proved. Precise fault location is the advantage of the presented MLP NN method, which causes quick restoration, maintenance and decrease unnecessary power

outage period. The results show that the estimation error is small and is within the permissible range. The proposed approach could be implemented in different LVDC systems.

## REFERENCES

- [1] Abdali, A., Noroozian, R., & Mazlumi, K. (2019). Simultaneous control and protection schemes for DC multi microgrids systems. *International Journal of Electrical Power & Energy Systems*, 104, 230-245. DOI: 10.1016/j.ijepes.2018.06.054.
- [2] F. Blaabjerg, R. Teodorescu, M. Liserre, and A. V. Timbus, "Overview of control and grid synchronization for distributed power generation systems," *IEEE Transactions on industrial electronics*, vol. 53, no. 5, pp. 1398–1409, 2006.
- [3] A. Abdali, K. Mazlumi and R. Noroozian, "Fast fault detection and isolation in low-voltage DC microgrids using fuzzy inference system," 2017 5th Iranian Joint Congress on Fuzzy and Intelligent Systems (CFIS), Qazvin, 2017, pp. 172-177. IEEE, DOI: 10.1109/CFIS.2017.8003678.
- [4] H. Nikkhajoei and R. H. Lasseter, "Distributed generation interface to the certs microgrid," *IEEE Transactions on Power Delivery*, vol. 24, no. 3, pp. 1598–1608, 2009.
- [5] F. Katiraei, R. Iravani, N. Hatziargyriou, and A. Dimeas, "Microgrids management," *IEEE Power and Energy Magazine*, vol. 6, no. 3, pp. 54– 65, 2008.
- [6] R. M. Cuzner and G. Venkataramanan, "The status of dc micro-grid protection," in *Industry Applications Society Annual Meeting, 2008. IAS'08. IEEE*, pp. 1–8, IEEE, 2008.
- [7] D. Salomonsson, L. Soder, and A. Sannino, "Protection of low-voltage dc microgrids," *IEEE Transactions on Power Delivery*, vol. 24, no. 3, pp. 1045–1053, 2009.
- [8] M. Saeedifard, M. Graovac, R. Dias, and R. Iravani, "Dc power systems: Challenges and opportunities," in *IEEE PES General Meeting*, pp. 1–7, IEEE, 2010.
- [9] P. Salonen, P. Nuutinen, P. Peltoniemi, and J. Partanen, "LVDC distribution system protection solutions, implementation and measurements," in *Power Electronics and Applications, 2009. EPE'09. 13th European Conference on*, pp. 1–10, IEEE, 2009.
- [10] T. Ericson, N. Hingorani, and Y. Khersonsky, "Power electronics and future marine electrical systems," in *Petroleum and Chemical Industry Technical Conference, 2004. Fifty-First Annual Conference* 2004, pp. 163–171, IEEE, 2004.
- [11] J. Ren, S. Venkata, and E. Sortomme, "An accurate synchrophasor based fault location method for emerging distribution systems," *IEEE Transactions on Power Delivery*, vol. 29, no. 1, pp. 297–298, 2014.
- [12] L. Tang and B.-T. Ooi, "Locating and isolating dc faults in multiterminal dc systems," *IEEE transactions on power delivery*, vol. 22, no. 3, pp. 1877–1884, 2007.
- [13] S. Azizi, M. Sanaye-Pasand, M. Abedini, and A. Hasani, "A traveling wave based methodology for wide-area fault location in multiterminal dc systems," *IEEE Transactions on Power Delivery*, vol. 29, no. 6, pp. 2552–2560, 2014.
- [14] J.-D. Park and J. Candelaria, "Fault detection and isolation in low voltage dc-bus microgrid system," *IEEE Transactions on Power Delivery*, vol. 28, no. 2, pp. 779–787, 2013.
- [15] J. Das and R. H. Osman, "Grounding of ac and dc low-voltage and medium-voltage drive systems," *IEEE Transactions on Industry Applications*, vol. 34, no. 1, pp. 205–216, 1998.
- [16] H. Iwamoto, K. Satoh, M. Yamamoto, and A. Kawakami, "High-power semiconductor device: a symmetric gate commutated turn-off thyristor," *IEEE Proceedings Electric Power Applications*, vol. 148, no. 4, pp. 363– 368, 2001.
- [17] H. Iwamoto, K. Satoh, M. Yamamoto, and A. Kawakami, "High-power semiconductor device: a symmetric gate commutated turn-off thyristor," *IEE Proceedings-Electric Power Applications*, vol. 148, no. 4, pp. 363– 368, 2001.

- [18] E. L. Wellner and A. R. Bendre, "Igcets vs. igbts for circuit breakers in advanced ship electrical systems," in 2009 IEEE Electric Ship Technologies Symposium, pp. 400–405, IEEE, 2009.
- [19] P. Steimer, O. Apeldoorn, E. Carroll, and A. Nagel, "Igcet technology baseline and future opportunities," in Transmission and Distribution Conference and Exposition, 2001 IEEE/PES, vol. 2, pp. 1182–1187, IEEE, 2001.
- [20] F. Luo, J. Chen, X. Lin, Y. Kang, and S. Duan, "A novel solid state fault current limiter for dc power distribution network," in Applied Power Electronics Conference and Exposition, 2008. APEC 2008. Twenty-Third Annual IEEE, pp. 1284–1289, IEEE, 2008.
- [21] W. Fei, Y. Zhang, and Z. Lu, "Novel bridge-type fcl based on self-turnoff devices for three-phase power systems," IEEE Transactions on Power Delivery, vol. 23, no. 4, pp. 2068–2078, 2008.
- [22] U. Ghisla, I. Kondratiev, and R. A. Dougal, "Branch circuit protection for dc systems," in 2011 IEEE Electric Ship Technologies Symposium, pp. 234–239, IEEE, 2011.
- [23] L. Fausett, *Fundamentals of neural networks: architectures, algorithms, and applications*. Prentice-Hall, Inc., 1994.
- [24] M. T. Hagan and M. B. Menhaj, "Training feed forward network with the Marquardt algorithm," IEEE Trans. on Neural Net., vol. 5, no. 6, pp.989-993, 1994.
- [25] Andersen, T. J. and Wilamowski, B.M. "A Modified Regression Algorithm for Fast One Layer Neural Network Training," World Congress of Neural Networks, Washington DC, USA, vol. 1, pp. 687- 690, July 17-21, 1995.
- [26] Battiti, R., "First- and second-order methods for learning between steepest descent and Newton's method," Neural Computation, vol. 4, no. 2, pp. 141-166, 1992.
- [27] A. Meghwani, S. C. Srivastava and S. Chakrabarti, "A Non-unit Protection Scheme for DC Microgrid Based on Local Measurements," in IEEE Transactions on Power Delivery, vol. 32, no. 1, pp. 172-181, Feb. 2017.
- [28] Song-Yi Lin and Chern-Lin Chen, "Analysis and design for RCD clamped snubber used in output rectifier of phase-shift full-bridge ZVS converters," in IEEE Transactions on Industrial Electronics, vol. 45, no. 2, pp. 358-359, Apr 1998.